

Supplementary Information for

Evolution of High-Molecular-Mass Hyaluronic Acid is Associated with Subterranean Lifestyle

Yang Zhao^{1, 2, #}, Zhizhong Zheng^{1, #}, Zihui Zhang¹, Yandong Xu², Eric Hillpot¹, Yifei S. Lin¹,
Frances T. Zakusilo¹, J. Yuyang Lu¹, Julia Ablaeva¹, Seyed Ali Biashad¹, Richard A. Miller³,
Eviatar Nevo⁴, Andrei Seluanov^{1, *}, Vera Gorbunova^{1, *}

1 Departments of Biology and Medicine, University of Rochester, Rochester, NY 14627, USA

2 Department of Physiology and Department of Hepatobiliary and Pancreatic Surgery of the First
Affiliated Hospital, Zhejiang University School of Medicine, Hangzhou 301158, China

3 Department of Pathology, University of Michigan Medical School, Ann Arbor, Michigan 48109,
USA

4 Institute of Evolution, University of Haifa, Haifa 3498838, Israel

These authors contributed equally to this work

* Corresponding authors:

Vera Gorbunova

Email: vera.gorbunova@rochester.edu

Andrei Seluanov

Email: andrei.seluanov@rochester.edu

This PDF file includes:

Supplementary Figures S1-7

Supplementary Figure legends

Other supplementary materials for this manuscript include:

Supplementary Data 1-3

Figure S1

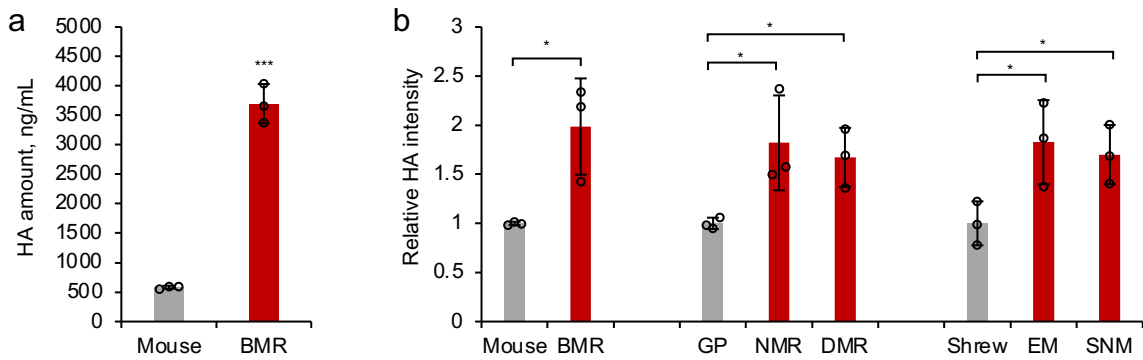


Fig. S1. Quantification of HA in conditioned media. (a) ELISA quantification of HA from media of BMR and mouse cells. Data are mean \pm SD of biological replicates. *** $P < 0.001$ by unpaired two-sided t-test. (b) Quantification of HA intensity from pulsed-field gel. HA purified from media of different cell lines was subjected to pulsed-field electrophoresis and stained with Stains-All. The relative HA intensity was quantified using ImageJ. Data are mean \pm SD of gels from three independent experiments. * $P < 0.05$ by unpaired two-sided t-test. Source data are provided as a Source Data file.

Figure S2

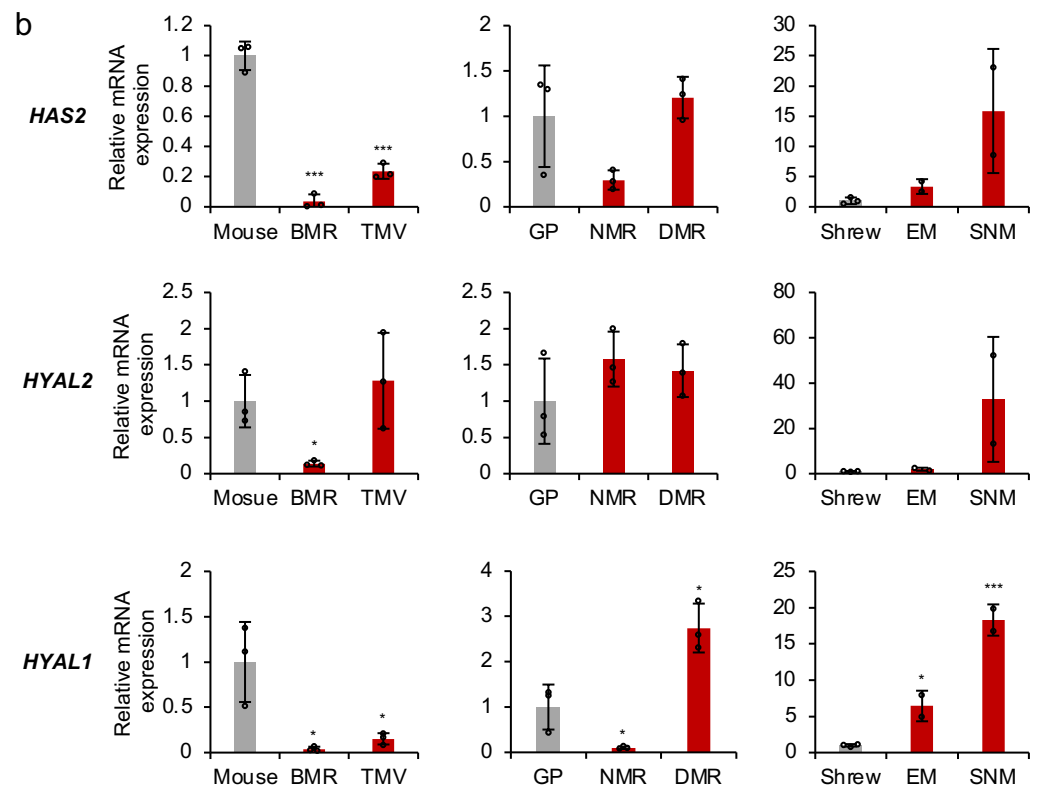
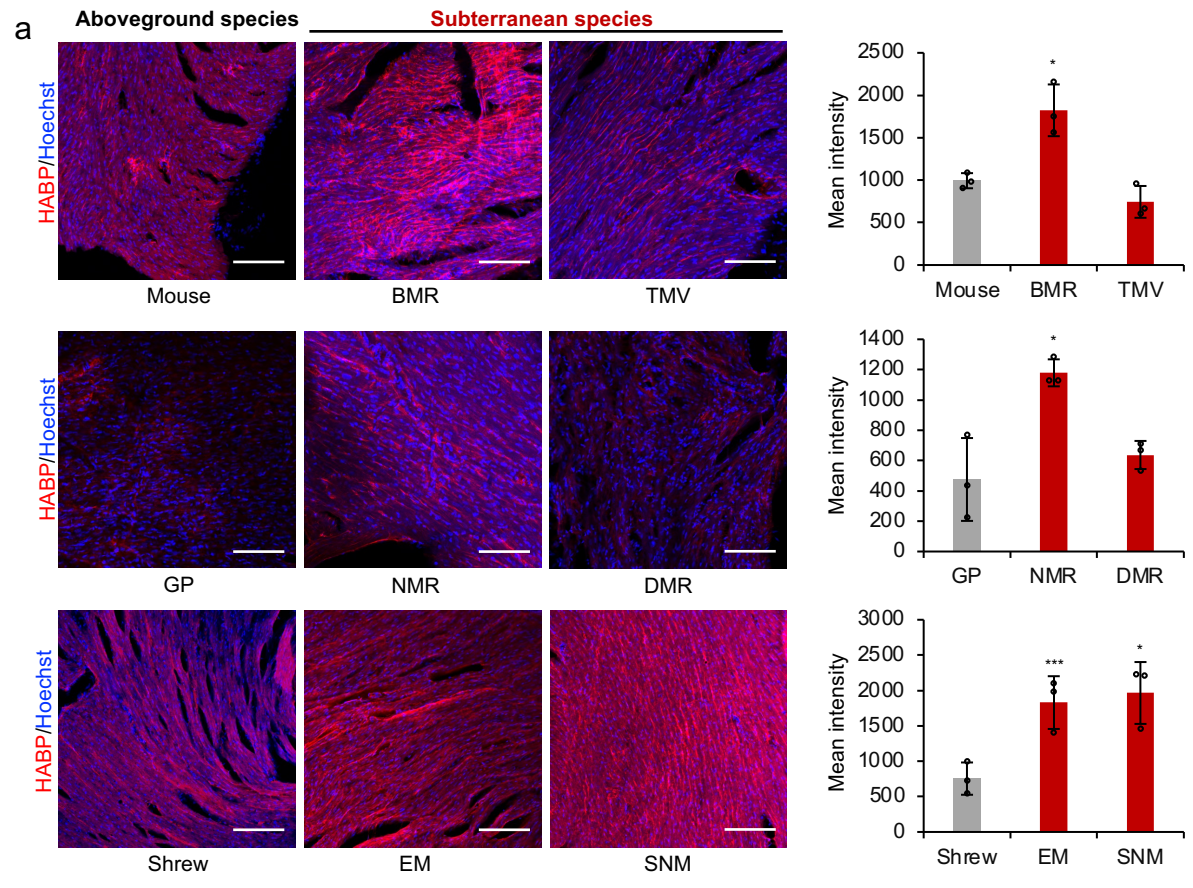


Fig. S2. Levels of HA in the heart of subterranean species. (a) Cryosections of heart tissues from different species were stained with hyaluronan binding protein (HABP, red) and Hoechst (blue). Experiments were repeated three times. Representative Immunofluorescence images are shown at 20 × magnification (left). Scale bar, 50 μm. Quantification of HABP fluorescence (right). Data are mean ± SD of three independent areas. *P*-value indicates the difference between subterranean and the corresponding aboveground species. * *P* < 0.05, *** *P* < 0.001 by unpaired two-sided t-test. (b) RT-qPCR showing expression levels of *HAS2* and *HYAL2* and *HYAL1* genes in the heart comparing subterranean species with their aboveground controls. Experiments were performed using three biological replicates, except EM and SNM, which had two biological replicates. *P*-value indicates the difference between subterranean and the corresponding aboveground species. Data are mean ± SD. * *P* < 0.05, *** *P* < 0.001 by unpaired two-sided t-test. Source data are provided as a Source Data file.

Figure S3

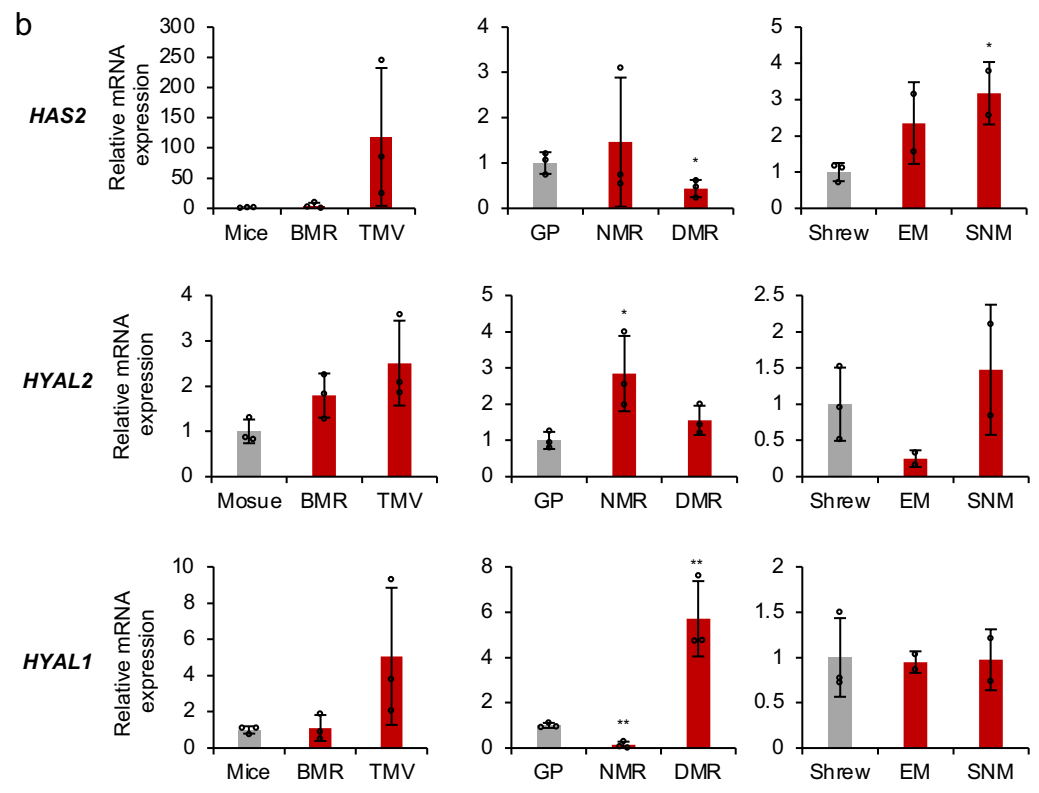
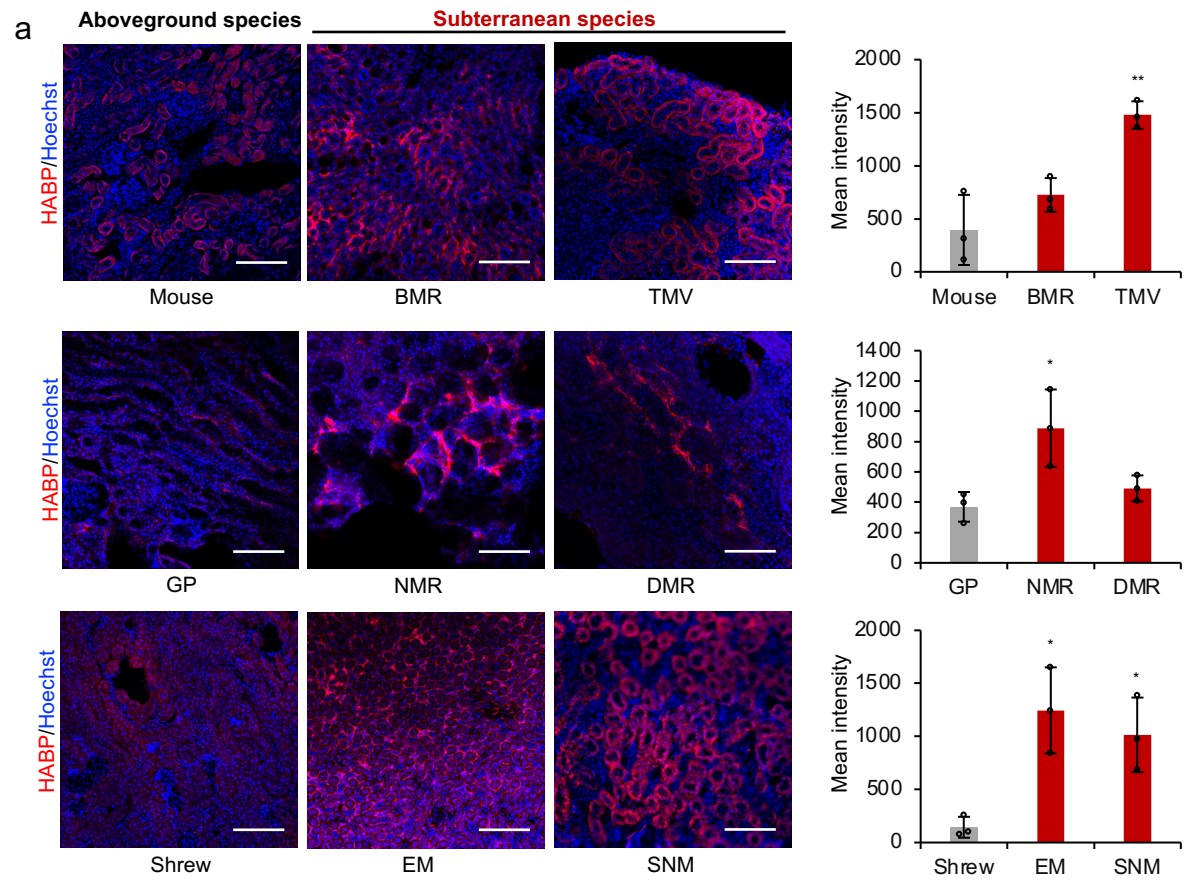


Fig. S3. Levels of HA in the kidney of subterranean species. (a) Cryosections of kidney tissues from different species were stained with hyaluronan binding protein (HABP, red) and Hoechst (blue). Experiments were repeated three times. Representative immunofluorescence images are shown at 20 × magnification (left). Scale bar, 50 μm. Quantification of HABP fluorescence (right). Data are mean ± SD of three independent areas. *P*-value indicates the difference between subterranean and the corresponding aboveground species. * *P* < 0.05, *** *P* < 0.001 by unpaired two-sided t-test. (b) RT-qPCR showing expression levels of *HAS2* and *HYAL2* and *HYAL1* genes in the heart comparing subterranean species with their aboveground controls. Experiments were performed using three biological replicates, except EM and SNM, which had two biological replicates. *P*-value indicates the difference between subterranean and the corresponding aboveground species. Data are mean ± SD. * *P* < 0.05, *** *P* < 0.001 by unpaired two-sided t-test. Source data are provided as a Source Data file.

Figure S4

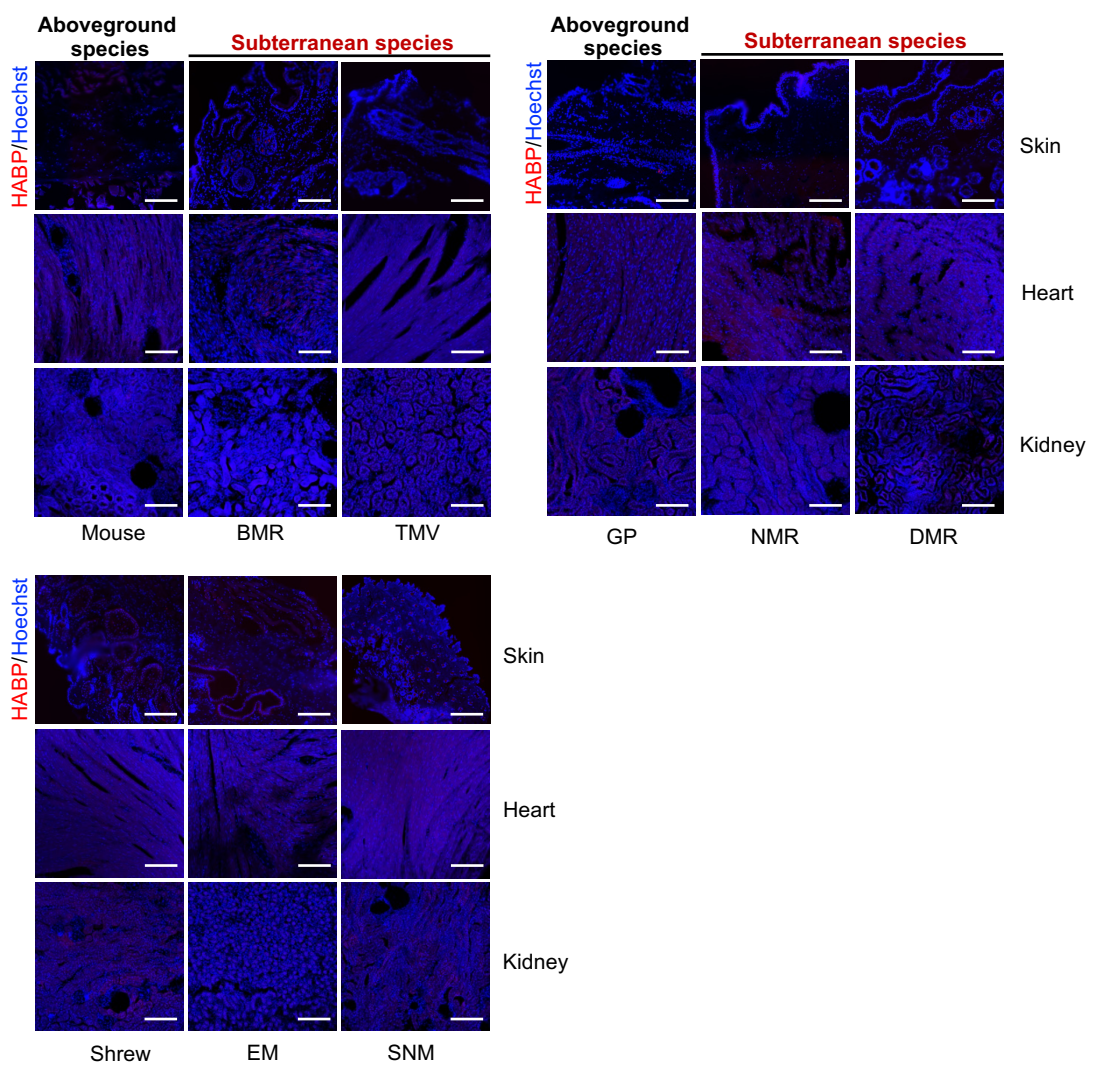


Fig. S4. Negative controls for tissue HABP staining. Cryosections of skin, heart, and kidney were treated with HAase overnight before staining with HABP. The negative signal for HABP channel indicates the specificity of HABP staining for HA. Scale bar, 50 μ m.

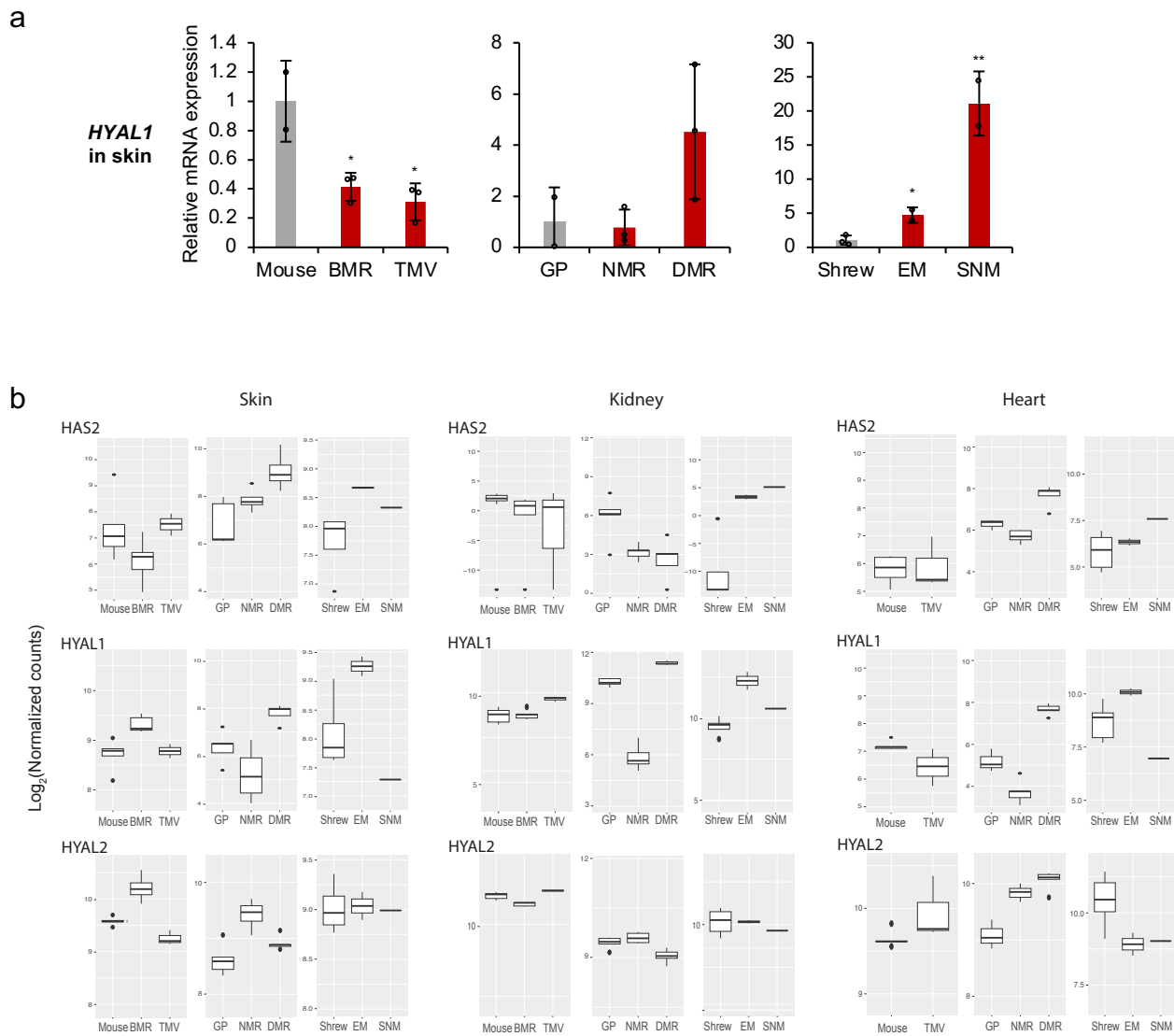
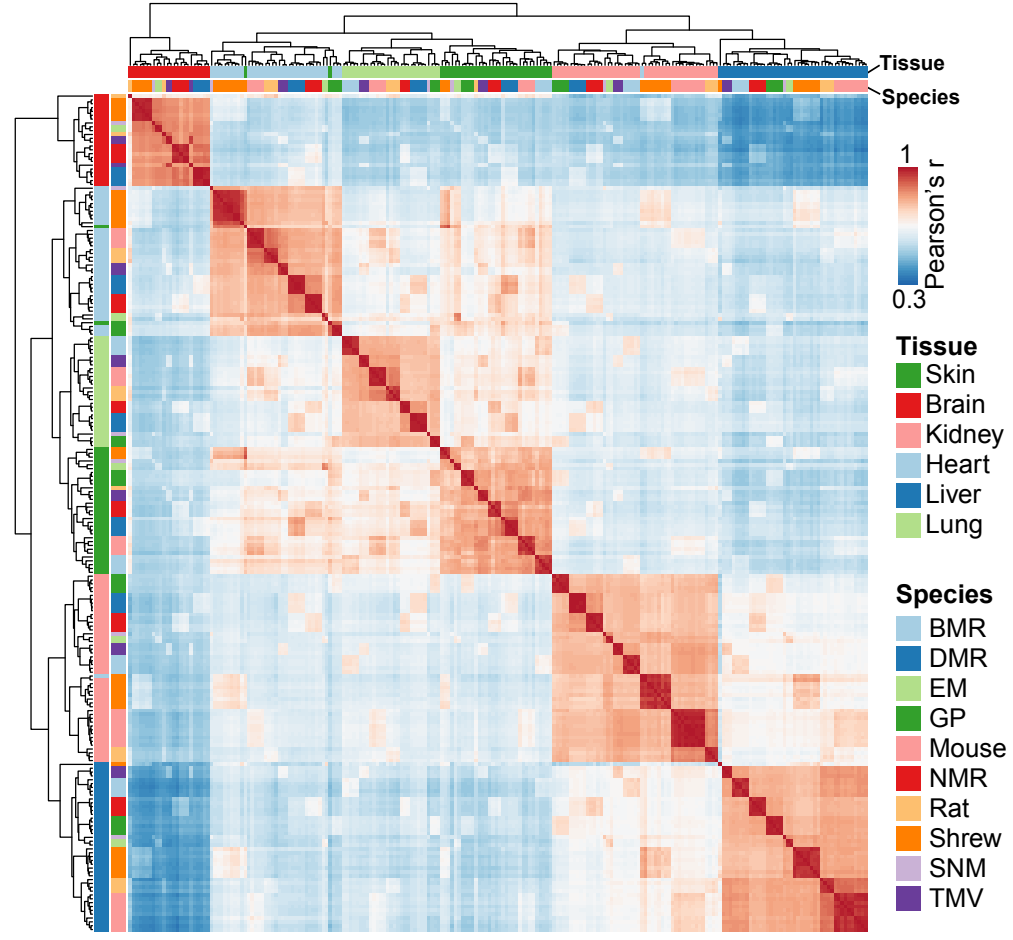


Fig. S5. Expression of HAS2, HYAL2, and HYAL1 in the tissues of subterranean species.

(a) RT-qPCR was performed using three biological replicates, except Mouse, GP, EM and SNM, which had two biological replicates. Data are mean \pm SD. * $P < 0.05$ by unpaired two-sided t-test. (b) Boxplots showing the expression of HAS2, HAYL1, and HYAL2 in skin, kidney and heart of different species determined by RNAseq. Log₂ transformed normalized counts were shown. The boxplots display the median, the 1st, and 3rd quartiles; the whiskers show a 1.5 \times interquartile range. Data points outside the whiskers are outliers. Skin: Mouse $n = 5$, BMR $n = 5$, TMV $n = 3$, GP $n = 5$, NMR $n = 4$, DMR $n = 5$, Shrew $n = 4$, EM $n = 2$, and SNM $n = 1$; Kidney: Mouse $n = 10$, BMR $n = 5$, TMV $n = 3$, GP $n = 5$, NMR $n = 5$, DMR $n = 5$, Shrew $n = 8$, EM $n = 2$, and SNM $n = 1$; Heart: Mouse $n = 5$, TMV $n = 3$, GP $n = 3$, NMR $n = 5$, DMR $n = 5$, Shrew $n = 10$, EM $n = 2$, and SNM $n = 1$. Source data are provided as a Source Data file.

Figure S6

a



b

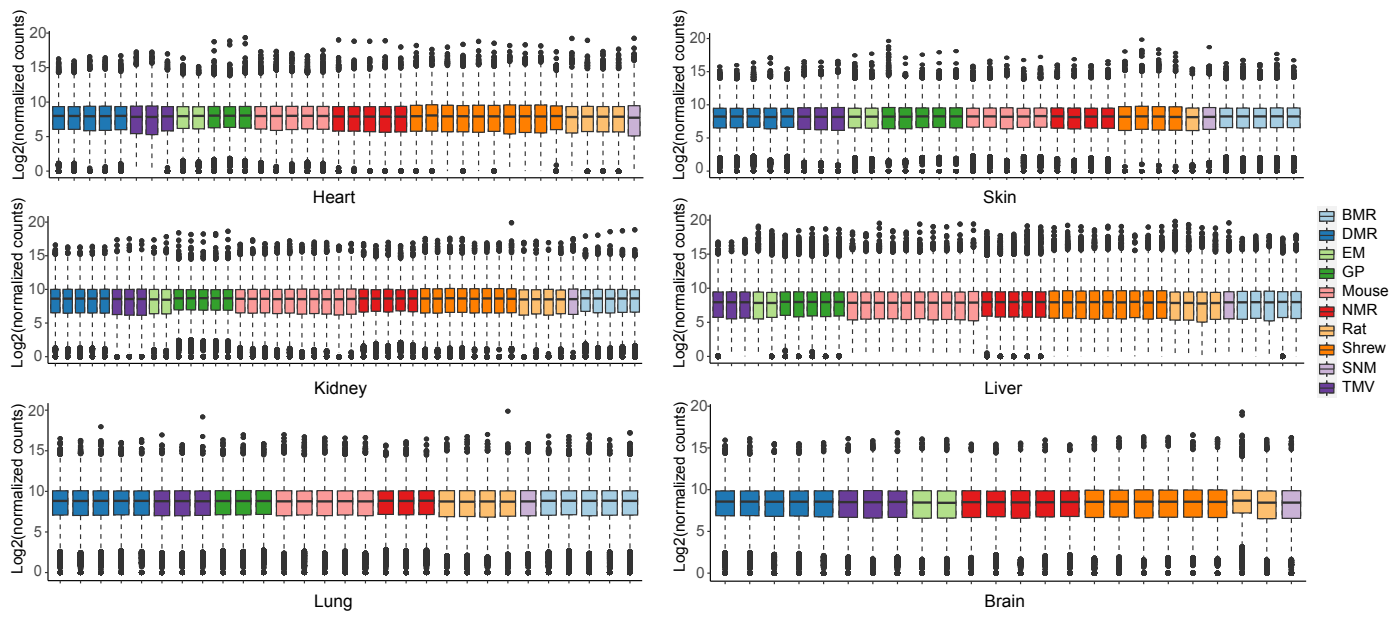
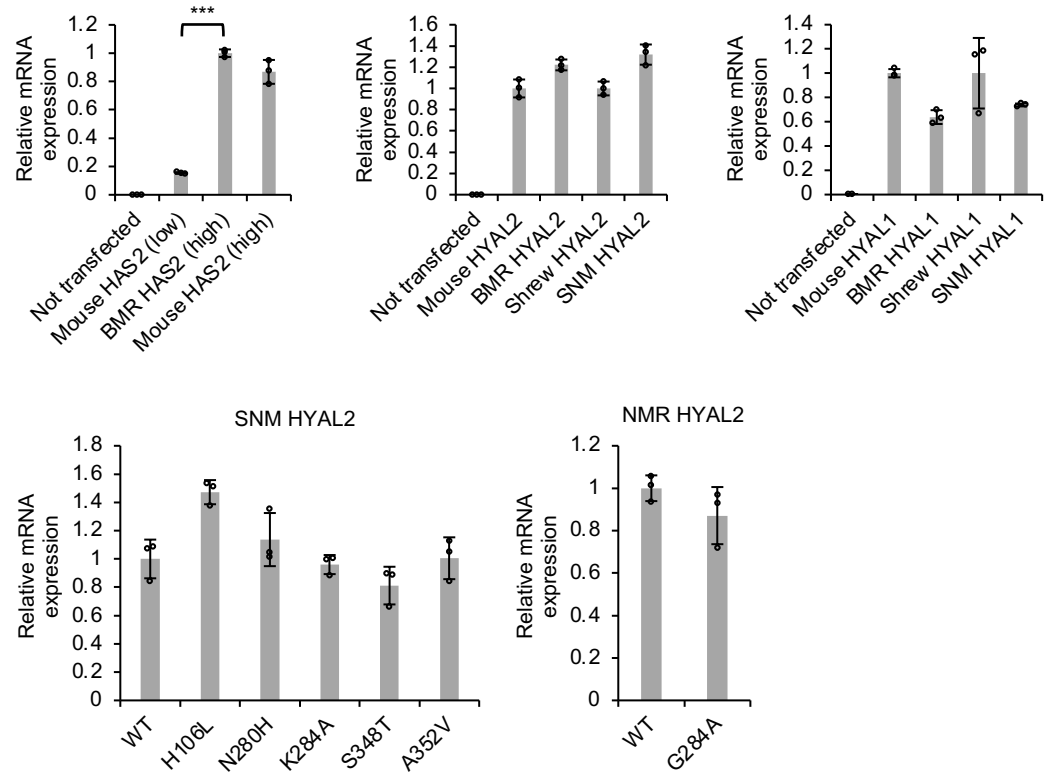


Fig. S6. Quality controls for RNA sequencing (RNAseq). (a) Heatmap showing the Pearson correlation coefficient among all samples. Samples are mainly clustered by tissues. (b) Boxplot of gene expression (in log scale) of individual samples for each tissue after filtering out low-expressed genes and normalized by DESeq2 package. The boxplots display the median, the 1st, and 3rd quartiles; the whiskers show a $1.5\times$ interquartile range. Data points outside the whiskers are outliers. Same number of genes were shown for each species: Heart $n = 13,089$, Kidney $n = 13,323$, Lung $n = 13,395$, Skin $n = 13,211$, Liver $n = 13,023$, and Brain $n = 13,452$.

Figure S7

a



b

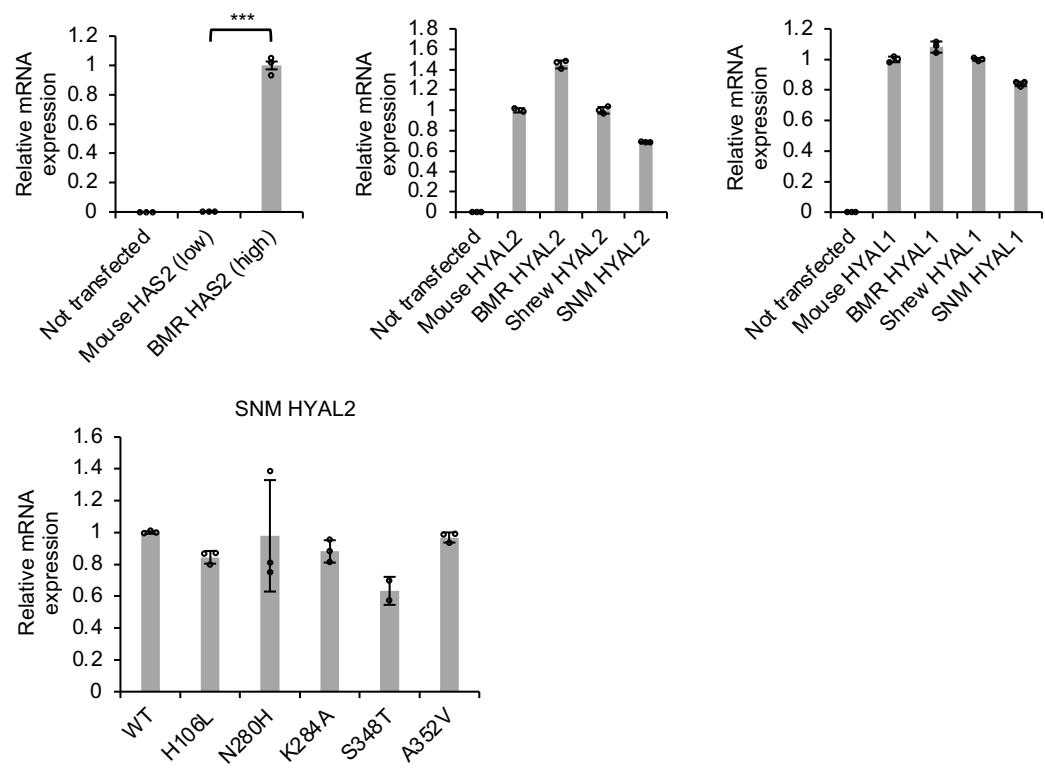


Fig. S7. Expression levels of transfected genes. HeLa cells (a) and 293T cells (b) were transfected with low amount of mouse HAS2 or high amount of BMR HAS2 to mimic the different endogenous expression in skin fibroblasts. Other genes including HYAL1 and HYAL2 from mouse, BMR, shrew, SNM, as well as mutant HYAL2 of SNM and NMR were transfected equally. RT-qPCR was performed to determine expression levels of HAS2, HYAL2, and HYAL1 in transfected cells. Data are mean \pm SD of three technical replicates. *** $P < 0.001$ by unpaired two-sided t-test. Source data are provided as a Source Data file.

Figure S8

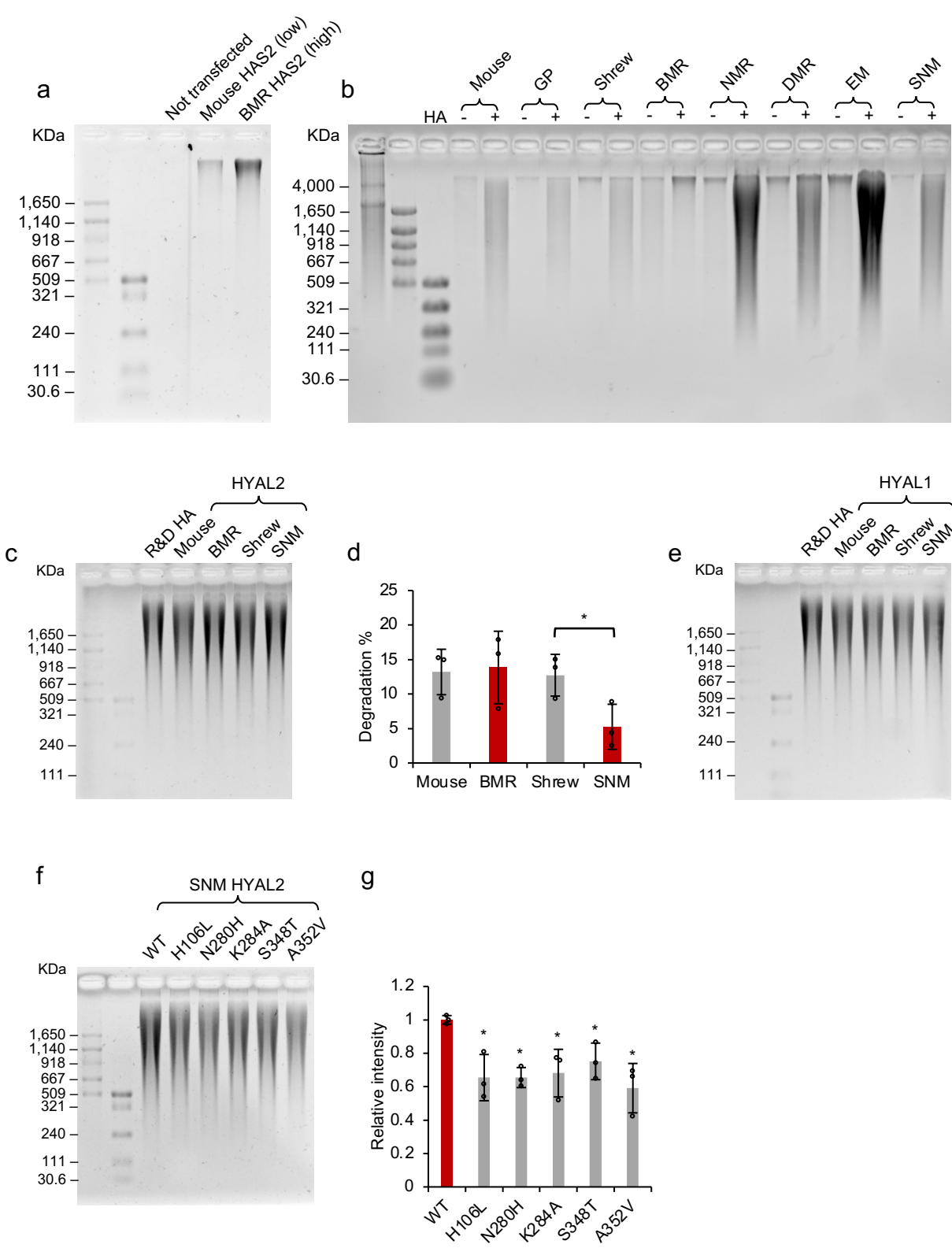


Fig. S8. Effects of HA-related enzymes on HA synthesis and degradation in subterranean species. (a) 293T cells were transfected with low amount of mouse HAS2 or high amount of BMR HAS2 (14-fold higher) plasmids. Two days after transfection, HA was purified and run on an agarose gel. (b) Media containing 20 $\mu\text{g}/\text{mL}$ commercial HMM-HA was incubated with growing fibroblasts from each species. Two days after incubation, HA was purified from the media and run on an agarose gel. For each cell line, a sample without commercial HA was included to control for the endogenous HA. The amount of loaded HA was normalized to cell number of each species. (c-e) 293T cells were transfected with either HYAL2 (c) or HYAL1 (e) of mouse, BMR, shrew, or SNM. Transfected cells were cultured in media containing 20 $\mu\text{g}/\text{mL}$ commercial HA. Two days after incubation, HA was purified and run on an agarose gel. (d) Quantification of HA gel in panel c. Degradation of HA by HYAL2 from different species was calculated based on the difference in intensity between R&D HA and the treated samples. HA intensities were quantified using ImageJ. (F) 293T cells were transfected with either wild-type (WT) SNM HYAL2 plasmid, or each of its five mutants. Cells were incubated with media containing 20 $\mu\text{g}/\text{mL}$ commercial HA for two days, followed by HA extraction and electrophoresis. (g) Quantification of HA intensities after degradation by WT or mutant SNM HYAL2. For (d) and (g), data are mean \pm SD of three technical replicates. * $P < 0.05$ by unpaired two-sided t-test. For (a), (b), and (e), experiments were performed three times with similar results. Source data are provided as a Source Data file.

Figure S9

a

```

Mouse 1  MHCERFLCVLRIIGTTLFGVSLLLGITAAYIVGYQFIQTDNYYFSFGLYGAF LASHLIIQSLFAFLEHRK 70
BMR 1    MHCERFLCILRIIGTTLFGVSLLLGITAAYIVGYQFIQTDNYYFSFGLYGAF LASHLIIQSLFAFLEHRK 70

Mouse 71  MKKSLETPIKLNKTVALCIAAYQEDPDYLRKCLQSVKRLTYPGIKVVVIDGNSDDDLYMMDIFSEVMGR 140
BMR 71  MKKSLETPIKLNKTVALCIAAYQEDPDYLRKCLQSVKRLTYPGIKVVVIDGNSDDDLYMMDIFSEVMGR 140

Mouse 141 DKSATYIWKNNFHEKGPGETEESHKESSQHVTQLVLSNKSICIMQKWGGKREVMYTAFRALGRSDYVQV 210
BMR 141 DISATYIWKNNFHEKGPGETDESHKESSQHVTQLVLSNKSVCIMQKWGGKREVMYTAFRALGRSDYVQV 210

Mouse 211 CSDTMLDPASSVEMVKVLEEDPMVGGVGGDVQILNKYDSWISFLSSVRYWMAFNIERACQSYFGCVQCI 280
BMR 211 CSDTMLDPASSVEMVKVLEEDPMVGGVGGDVQILNKYDSWISFLSSVRYWMAFNIERACQSYFGCVQCI 280

Mouse 281 SGPLGMYRNSLLHEFVEDWYNQEFMGNQCSFGDDRHLTNRVLSLGYATKYTARSKCLTETPIEYLRWLNQ 350
BMR 281 SGPLGMYRNSLLHEFVEDWYNQEFMGNQCSFGDDRHLTNRVLSLGYATKYTARSKCLTETPIEYLRWLNQ 350

Mouse 351 QTRWSKSYFREWLYNAMWFHKHLLWMTYEAVITGFFPFLLIATVIQLFYRGKIWNILLFLLTVQLVGLIK 420
BMR 351 QTRWSKSYFREWLYNAMWFHKHLLWMTYEAVITGFFPFLLIATVIQLFYRGKIWNILLFLLTVQLVGLIK 420

Mouse 421 SSFASCLRGNIVMFMSLYSVLYMSSLLPAKMFAIATINKAGWGTSGRKTIVVNFIFGLIPVSVWFTILLG 490
BMR 421 SSFASCLRGNIVMFMSLYSVLYMSSLLPAKMFAIATINKAGWGTSGRKTIVVNFIFGLIPVSVWFTILLG 490

Mouse 491 GVIFTIYKESKKPFSESKQTVLIVGTLIYACYWVMLLTLYVVLINKCGRRKKGGQQYDMVLDV 552
BMR 491 GVIFTIYKESKKPFSESKQTVLIVGTLIYACYWVMLLTLYVVLINKCGRRKKGGQQYDMVLDV 552
  
```

b

NID1

	I198V	D982E
Consensus	KSDGAYNIFANDRES	YWTDWNRDNPKIETS
BMR	RT V
Zokor	. TN V
Bamboo rat	RT V
TMV	S . N . Y . TV ES
Mouse	. . N
Rat	. . N
Kangaroo rat	. . . P D . Q D
NMR V SK
DMR V SK E
GP	. . . V SK
Human	. . N
SNM	S . N . TV . V . . E . A ER A
EM	. . N . TF K S
Shrew	. . N . VH ES
Dog	. . E S
Elephant	. T S A
Armadillo S

Fig. S9. Alignment of HAS2 and NID1 protein sequence. (a) Alignment of mouse and BMR HAS2 protein sequences. (b) Locations of two convergent mutation sites of NID1 protein across subterranean species are indicated with arrows. The names of subterranean species are labeled in red.

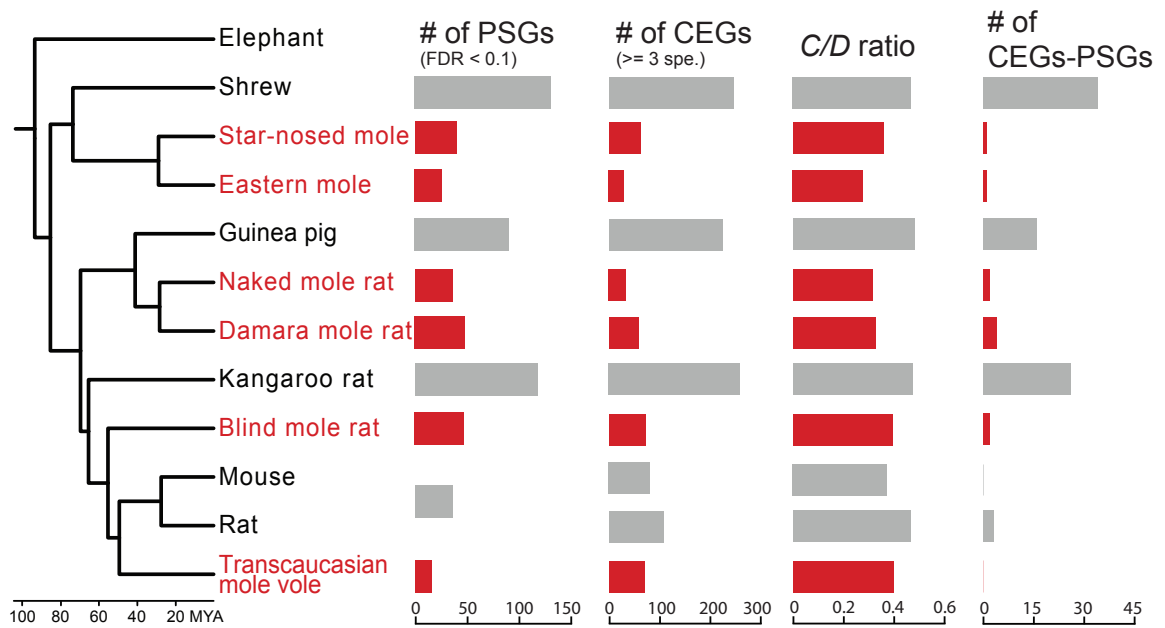


Fig. S10. Positively selected and convergently evolving genes in subterranean species.

Phylogenetic tree of species without plateau zokor and hoary bamboo rat and their numbers of positively selected genes (PSGs), convergently evolving genes (CEGs), convergent-to-divergent site ratio (*C/D* ratio; ≥ 3 species) and genes with both positive selection sites and convergent sites (CEGs-PSGs). Error bars indicate the standard deviations of numbers of CEGs and *C/D* ratio resulting from different combinations of species. Subterranean species are shown in red.

Figure S11

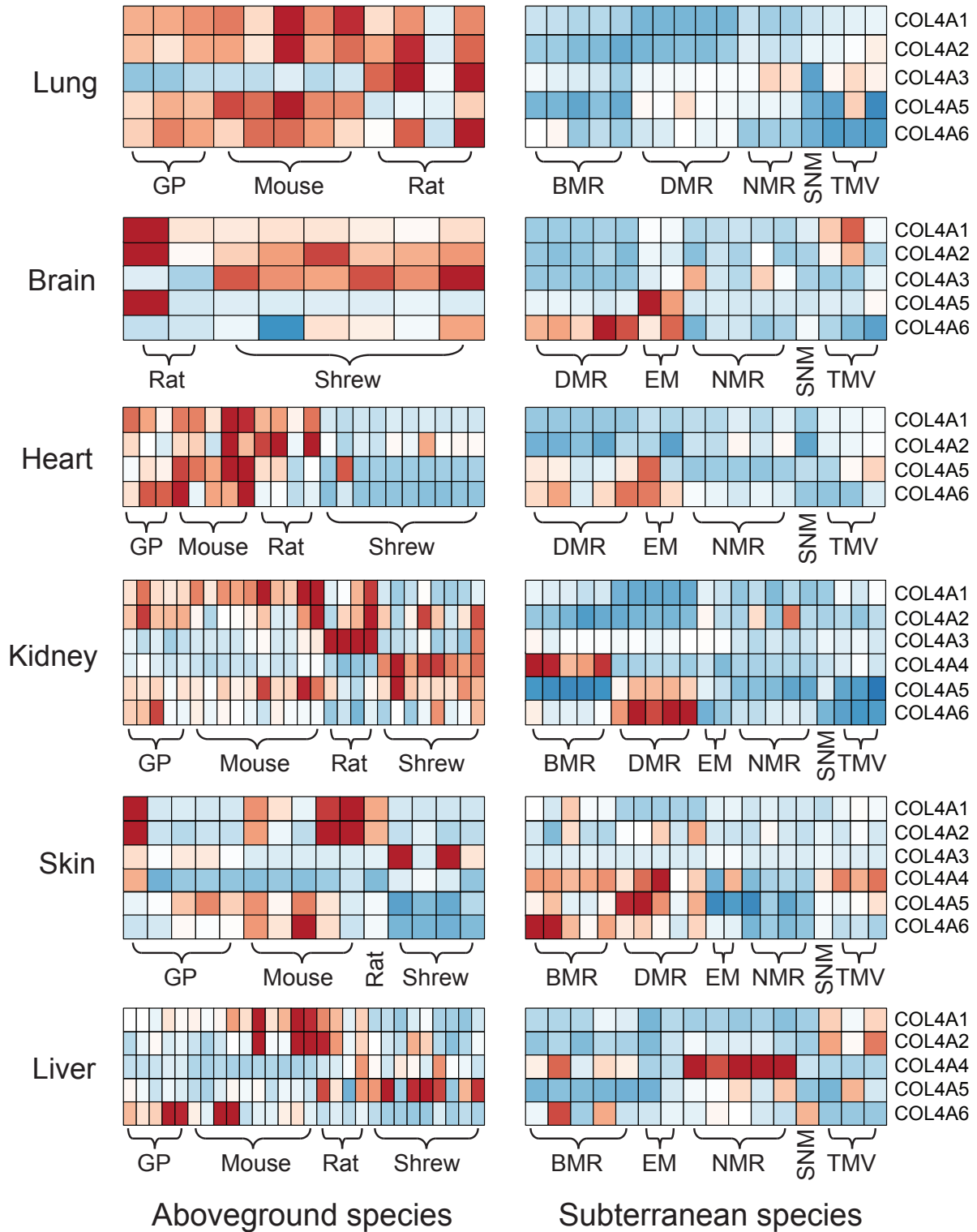


Fig. S11. The heatmap showing expression of type IV collagen genes between subterranean and aboveground species. Heatmap showing expression of six genes including COL4A1, COL4A2, COL4A3, COL4A4, COL4A5 and COL4A6. COL4A1 and COL4A2 show consistently lower expression in most of the subterranean species in the lung, brain, heart, and kidney, but not in skin and liver.